EXPERIMENTAL INVERSITIGATION OF TOLLMIEN SCHLICHTING INSTABILITY AND TRANSITION IN SIMILAR BOUNDARY LAYER FLOW IN AN ADVERSE PRESSURE GRADIENT

by

F.J.M. Wubben
D.M. Passchier
J.L. van Ingen

Note: The results of a two-dimensional experiment are described, performed in the similar laminar and transitional part of a boundary layer flow (Hartree β=-.14) under natural disturbance conditions. At 23 streamwise stations mean velocity profiles, power spectra, power distributions across the boundary layer and amplification spectra are measured and compared with boundary layer- and linear stability calculations.

Experimental Investigation of Tollmien Schlichting Instability and Transition in Similar Boundary Layer Flow in an Adverse Pressure Gradient

F.J.M. WUBBEN, D.M. PASSCHIER, J.L. VAN INGEN

Low Speed Aerodynamics Laboratory (LSL)
Department of Aerospace Engineering
Delft University of Technology
The Netherlands

SUMMARY
The results of a two dimensional experiment are described, performed in the similar laminar, and transitional part of a boundary layer flow (Hartree β= −0.14) under natural disturbance conditions. At 23 streamwise stations, mean velocity profiles, power spectra, power distributions across the boundary layer and amplification spectra are measured and compared with boundary layer- and linear stability calculations.

INTRODUCTION

In 1986, due to the increased interest in natural laminar flow (NLF) and laminar flow control (LFC), an experimental project was started at LSL to investigate the region of validity of linear stability theory in natural boundary layer flows. The investigations were performed at LSL on the flat test wall of a small boundary layer tunnel, with a flexible opposite wall to generate a pressure gradient. Except for a short initial pressure region, the pressure distribution corresponded to a Hartree β = −0.14 flow (figure 1).
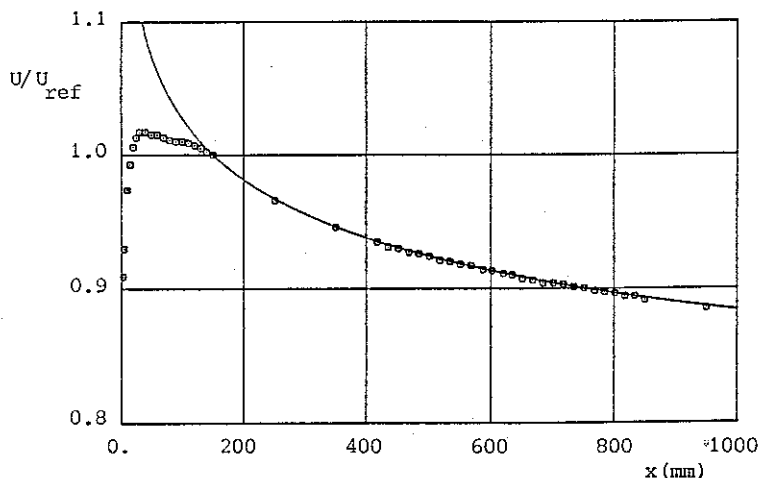

Figure 1. Experimental (⊙) and theoretical (—) velocity distribution, Hartree β = −0.14 ($\bar{U}_{ref}$ = 10.96 m/s).

Experimental results were compared with two quasi-parallel linear stability computer programs. The first is part of the low speed airfoil analysis and design code of LSL (Van Ingen et al. [1]). The method uses spatial linear stability data for the similar Falkner Skan (Hartree) mean velocity profiles, which were read from small scale charts, and solutions of the Rayleigh equation for the inviscid stability of reversed flows (as occurring in separation bubbles). All these data have been reduced to a table containing about 600 numbers.

The second program is a finite difference compressible temporal linear stability code, based on Cosal (Malik [2]), of the National Aerospace Laboratory (NLR).

EXPERIMENTAL SET-UP

All experiments were performed on the flat test wall of an open ended boundary layer windtunnel with a contraction ratio of 16.7 and a 2 m long test section. The entrance of the rectangular test section has dimensions 0.08 x 0.48 m. Downstream, variable cross sections can be obtained with a flexible transparant PVC counter wall. Suction was employed to keep the boundary layer growth on the opposite wall within bounds. The pressure distribution was measured with 41 pressure orifices fitted in two stream-wise rows along the test wall.

A single tungsten hot wire with 1 mm active length and 5 μm diameter was used, connected to a Dantec (56C01) constant temperature anemometer with an overheat ratio of 0.8. Mean voltages were measured with a Fluke (8842A) digital voltmeter. A DISA bandpass filter with frequency band 5-2000 Hz and roll-off rate 18 dB/octave, was used to obtain the fluctuating part of the signal which was analysed by a Bruel & Kjaer (type 2031) narrow band frequency analyser. Voltmeter and analyser data were read out by an HP-1000 computer and stored on disk and magnetic tape.

All measurements were performed at a free stream reference speed of 10.96 m/s (see figure 1) and a free stream turbulence intensity of 0.05%, half of which was contributed by disturbances below 25 Hz.

RESULTS AND DISCUSSION

Mean velocity profiles

Boundary layer measurements were performed at 23 locations along the test wall in the laminar and transitional region of the flow. Comparison of the experimental mean velocity profiles with the Hartree β = -0.14 profile showed a good correspondence downstream of x = 250 mm where the effects of the non-Hartree initial region were damped out. Experimental laminar mean velocity profiles were also compared with Bola (Lindhout et al.[3]), a finite difference boundary layer code of NLR. Differences were mainly due to errors in the experimentally determined wall distance of the hot wire,
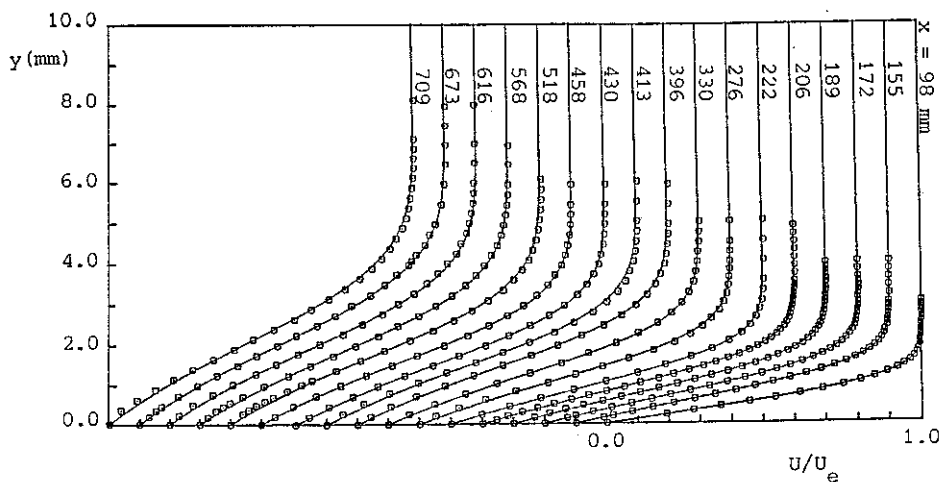
Figure 2. Development of boundary layer. Comparison between experiment (⊙) and Bola results (—).

also observed in comparisons of the measured and calculated displacement thickness. The calculated profiles were used to adjust the measured wall distance, to obtain a better fit. These corrections were applied in all laminar results ($x \leq 709$ mm) and were in general less than 0.05 mm. The laminar boundary layer development, compared with Bola results, is presented in figure 2. Agreement is quite satisfactory except for some local regions close to the wall, attributed to local deviations in the experimental pressure gradient, not accounted for in the calculations.

Figure 3 presents the shape factor, in the laminar part also compared with Bola results. The figure shows the transition region to extend from about 700 mm till 900 mm.

Power spectra

Over 800 power spectra were measured at 19 boundary layer stations in the laminar and transitional flow region (these can be made available on floppy disk to the interested reader). The voltage power spectra measured with the frequency analyser covered a frequency band of 0-1000 Hz, subdivided in 400 intervals of 2.5 Hz each. Those voltage power spectra were reduced to velocity power spectra by means of the sensitivity of the hot wire anemometer. The anemometer signal representing the instantaneous velocity is contaminated by electronic noise and other disturbing signals. They are not correlated with the flow velocity but are treated as if representing a velocity during data reduction. Figure 4.a shows voltage power spectra at three levels in the boundary layer at $x = 276$ mm from which three kinds of disturbances may be distinguished.
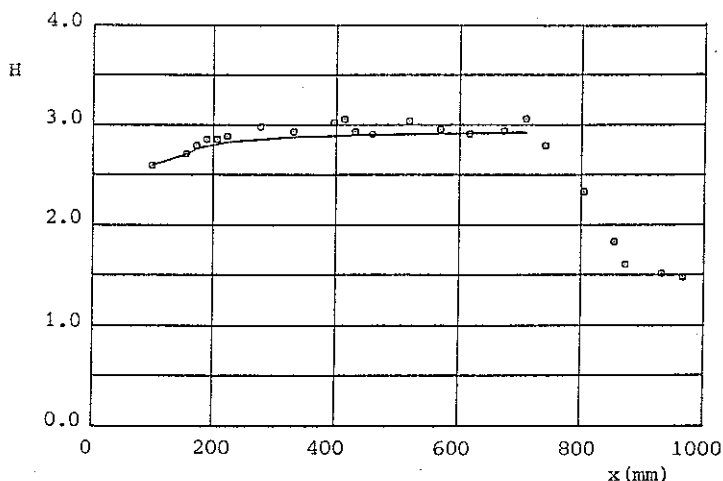
Figure 3. Distribution of shape factor. Experiments (⊙), Bola results (—).

The first disturbances are of a velocity- (or pressure) nature like the peaks at 320 Hz corresponding to the fan blade frequency and its harmonic at 640 Hz, and the motor sound at 612.5 Hz. Their intensity is nearly independent of the wall distance in a velocity power spectrum (figure 4.b). The second are electronic noise like the peaks at the electric mains frequency (50 Hz) and its harmonics, and the white noise in between. Their intensity is nearly independent of the wall distance in a voltage power spectrum (figure 4.a), and scale in a velocity power spectrum (figure 4.b), due to the data reduction procedure, with the inverse of the corresponding anemometer sensitivity.

At low frequencies (< 30 Hz), large power contributions are present which do not damp nor amplify downstream and strongly resemble the high fluctuation levels at very low frequencies in open jet facilities (Meier et al. [4] and Michel and Froebel [5]).

Spectra are presented at a limited number of representative boundary layer stations in figures 5 (Wubben [6] gives more details). They are given close to $(y/\theta) = 0.7$ and 2.8 at which maxima in power distributions (in the frequency band 25-200 Hz) were observed. Notice that the edge of the Hartree boundary layer is at $(\delta_{99}/\theta) = 7.37$. The free stream spectrum, $(y/\theta) > 20$, is presented as reference for spectra within the boundary layer.

At $x = 330$ mm, a clear hump can be observed at about 190 Hz, representative for TS-frequencies. Further downstream, the hump slowly shifts to lower frequencies and increases in magnitude. At $x = 430$ mm, a second hump appears around 100 Hz which seems to resemble the experiments of Kachanov
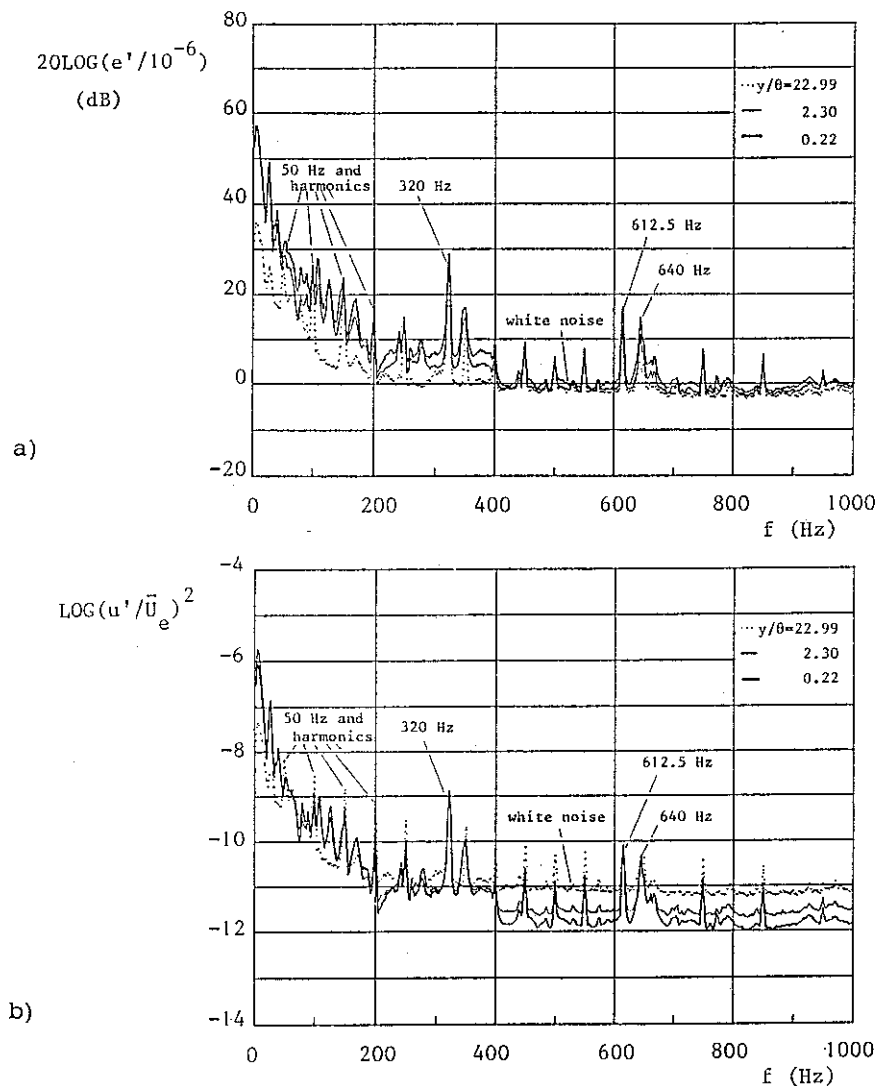
Figure 4. Voltage- (a) and velocity (b) power spectra at three levels in the boundary layer (x = 276 mm).

et al ([7] and [8]), possibly corresponding to subharmonics (half the frequency) of TS-waves. Because in the present experiment attention was focussed on the amplification of natural disturbances, there is no clear way of distinction between TS-waves and subharmonics.

At x = 518 mm, above 200 Hz, only disturbing contributions are observed in the spectra. An interesting change in this behaviour can be observed in the spectra at x = 616 mm (see also next paragraph). It will be evident that noise no longer dominates the signal. The same phenomenon was observed in
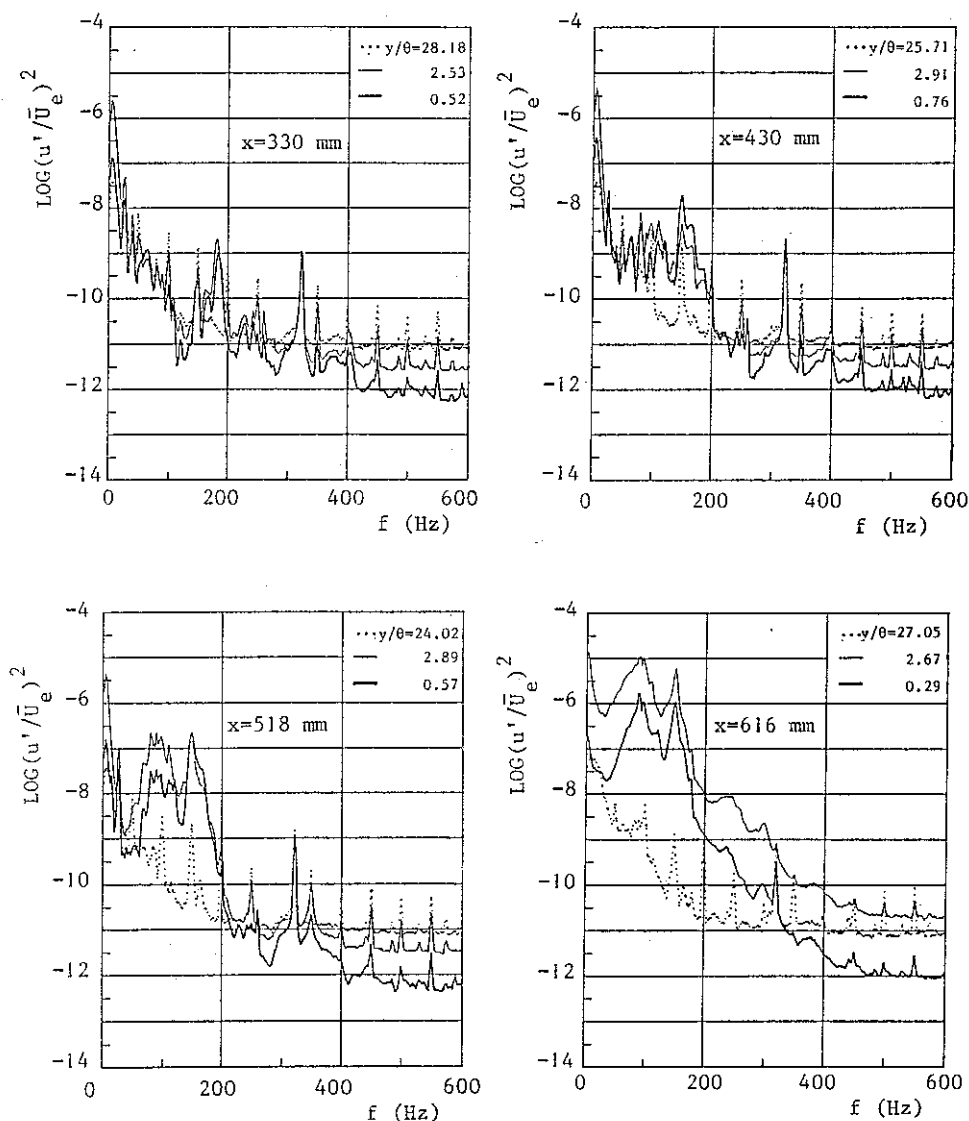
Figure 5. Development of velocity power spectra.

the experiments of Kachanov et al. [7] due to interaction processes between low frequency disturbances ($f < f(TS)$) and TS-waves which is the start of the filling of the spectrum to turbulence.

At $x = 709$ mm, where clear differences between the experimental and calculated mean velocity profiles were seen for the first time, all spectral components grow. Oscillograms showed the typical intermittency phenomenon characterized by high frequency fluctuations alternating with more regular laminar flow.
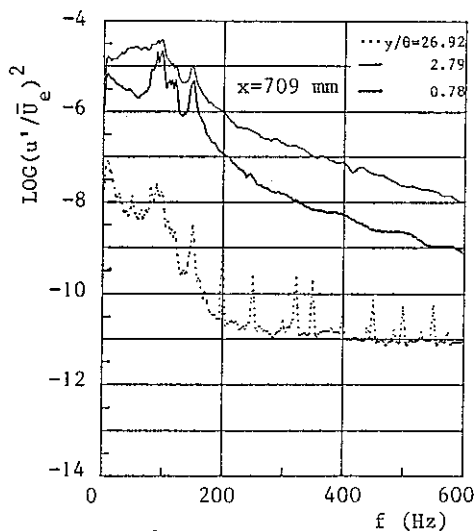
Figure 5. Continued.

Power distributions across the boundary layer

Because the total RMS-value is contaminated by disturbing signals, the power content in smaller frequency bands was analysed trying to avoid the disturbance peaks. These data were obtained from the measured power spectra.

Starting with the frequency band 155-195 Hz, figure 6 shows the experimental distribution compared with Cosal results at 175 Hz. Because the calculated amplitude distributions are normalized, the computed results are matched to the experiment, at the arrow. The boundary layer edge (δ_{99}/θ) is indicated as b.e.

At x = 330 mm, large differences are present due to the low signal to noise ratio at this station. Downstream, agreement is much better be it that differences can be observed in the free stream. This is due to the boundary condition of the Orr Sommerfeld equation at infinity, not taking into account the free stream turbulence. At x = 518 mm, an additional maximum is present in the experimental results, growing downstream, not found from the present linear stability calculation. Maxima are named A, B and C with increasing wall distance.

Similar conclusions can be drawn from the distributions in the frequency band 105-145 Hz, not shown here. However, the additional (B-)maximum is observed much earlier and is the absolute maximum from the very start.

At still smaller frequencies, the maximum is growing while in the band 25-45 Hz only the B-maximum is left over. This trend is also shown in figure 7

which presents power distributions in four frequency intervals at
x = 518 mm.

It should be noted that a B-maximum in the amplitude distribution is known
from a linear stability calculation (Arnal [9]) but is found only at
stronger adverse pressure gradients, by inflectional instability.

The experimental B-maximum becomes more and more dominant at lower fre-
quencies. From references [7] and [8] it is known that subharmonic maxima
are found close to the critical layer. So the B-maximum, observed in the
experiment, may possibly be related to subharmonic oscillations (Herbert
and Bertolotti [10]).

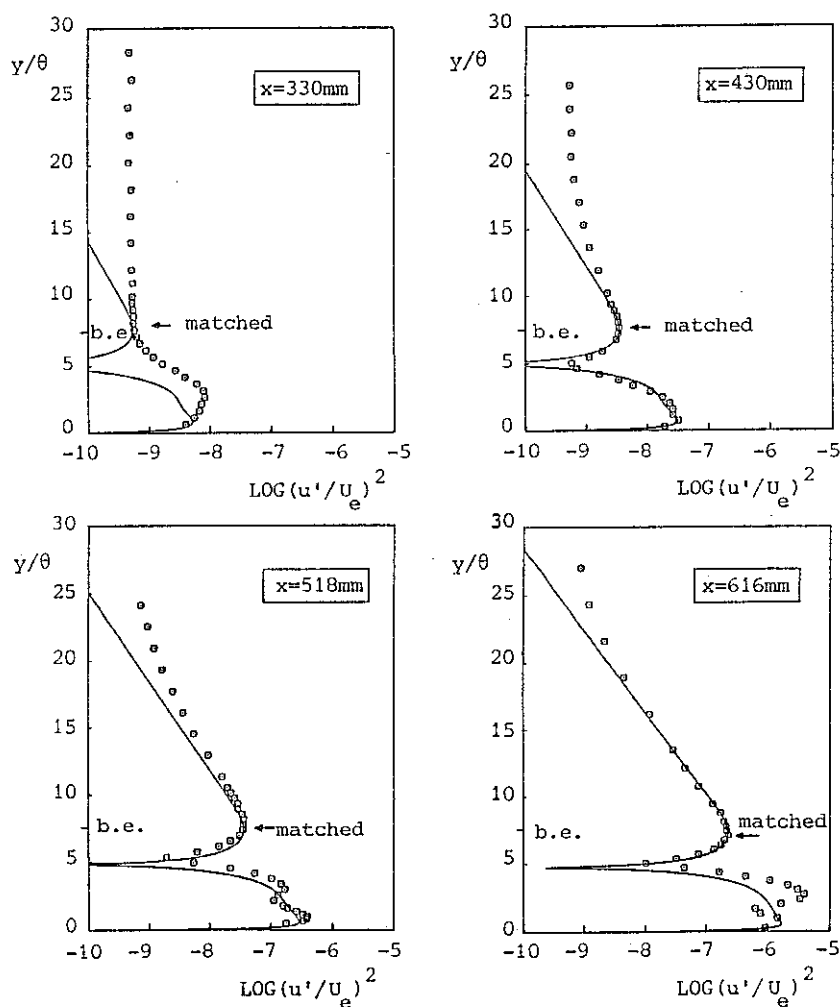As discussed in the previous paragraph, an interesting change was observed

Figure 6. Development of experimental power distribution (⊙ , 155-195 Hz)
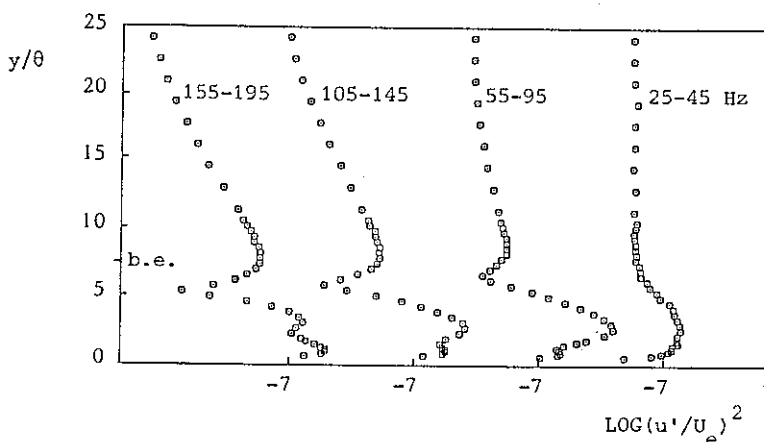compared with matched Cosal results (——, 175 Hz).

Figure 7. Experimental power distributions for different frequency intervals at x = 518 mm with shifted origins.

in the spectra above 200 Hz, at boundary layer station x = 616 mm. To demonstrate this change across the boundary layer, power distributions were determined at the frequency band 505–545 Hz (figure 8), at small x-values dominated by noise. Because the voltage power in this frequency band changes only little across the boundary layer at these small x-values, the presented distributions are directly proportional to the inverse of the hot wire sensitivity.

At x = 616 mm, a discontinuity is visible in the distribution, located at the boundary layer edge. The same phenomenon was seen at x = 568 mm, not presented here, close to the inflexion point in the mean velocity profile. It appears that the power content in the boundary layer increases suddenly when approaching the wall. So it seems that possible interaction processes between low frequency oscillations and TS-waves, at first, remain confined to only a part of the boundary layer. Downstream, the whole boundary layer is affected.
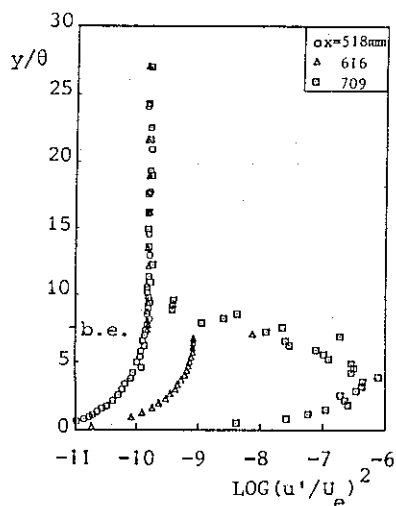

Figure 8. Development of experimental power distributions (505–545 Hz).

Amplification spectra

Although similar mean velocity profiles are present in the laminar flow, power distributions of disturbances change downstream due to the changing Reynoldsnumber $R_{\delta*}$, and are frequency dependent. The question to be raised is: which path through the boundary layer should be chosen to determine amplification? In general, amplification is calculated along
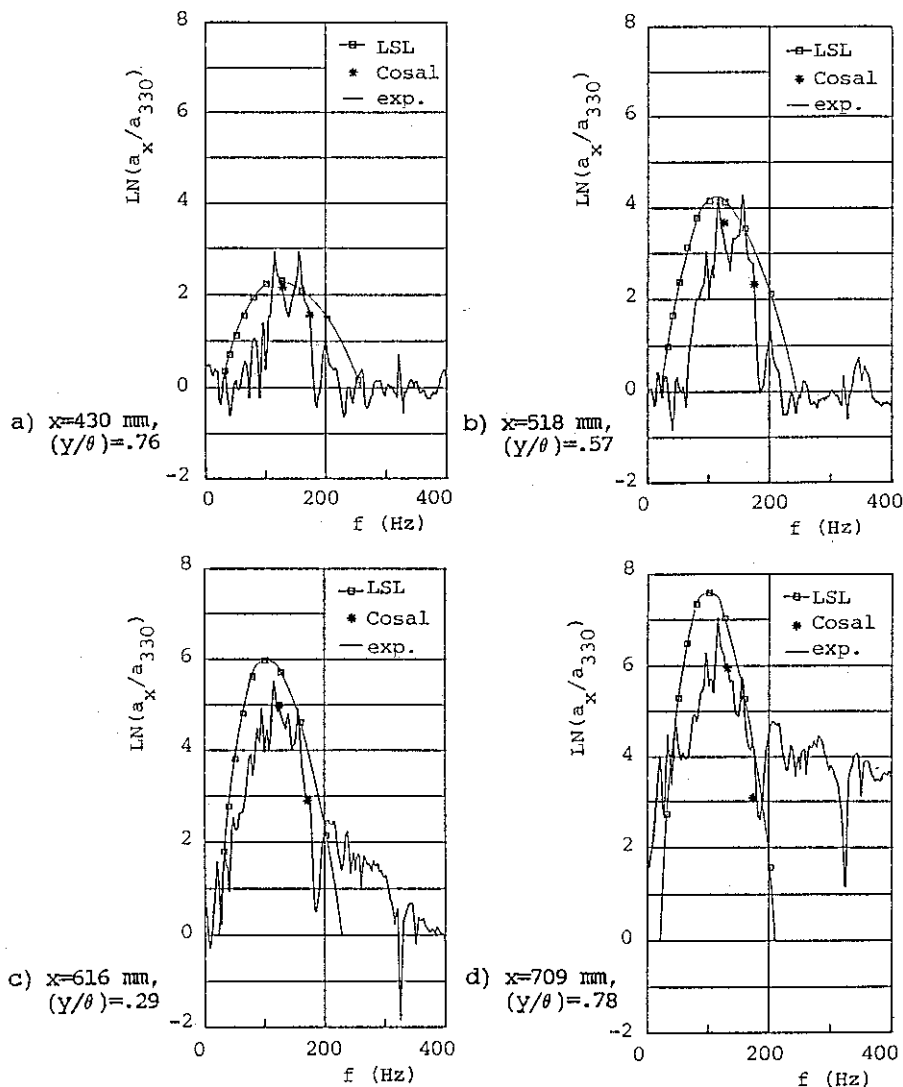

a) x=430 mm, (y/θ)=.76

b) x=518 mm, (y/θ)=.57

c) x=616 mm, (y/θ)=.29

d) x=709 mm, (y/θ)=.78

Figure 9. Amplification spectra. Amplification is with respect to the spectrum, measured at x = 330 mm and y/θ = .52. At x = 330 mm, a calculated "n factor" of 5 is found. Hence, figure 9b shows an n factor of about 9 (n = $LN(a_x/a_o)$).

lines of $|u'|_{max}$ or constant η, which is the non-dimensional Falkner Skan wall distance. However, the maximum is generally found at different wall distances for different frequencies. Therefore, a kind of average path was considered, along which the maximum intensity of all unstable waves (in the frequency band 25-200 Hz) together, evolved. This path appeared to be very close to lines of constant η (or y/θ). Hence, amplification data were reduced from spectra measured closest to constant (y/θ).

Amplification data have been presented with reference to the disturbance amplitudes at a reference station ($x = 330$ mm) rather than using some ill-defined initial amplitude which is dominated by noise. Because the signal to noise ratio at the reference station is still relatively small, the observed amplification at downstream stations, will be lower than the actual growth. Amplification spectra, reduced from spectra measured closest to (y/θ) = 0.7 are presented in figures 9. Linear stability results calculated with the LSL table and Cosal are included. It should be remarked that these last results are independent of the path through the boundary layer.

Initially, experimental amplification exceeds the predictions, downstream however, reversed trends are visible. The figures clearly show an overprediction of the LSL table while Cosal gives reasonable agreement. The LSL code also presents a wider unstable frequency band than the experiments.

Comparison of amplification spectra composed at (y/θ) = 2.8 (which is the average location of the additional (B-)maximum) with the presented amplification spectra showed a tendency to shift the amplification to lower frequencies, strengthening the believe that this maximum is of a subharmonic nature (figure 10).
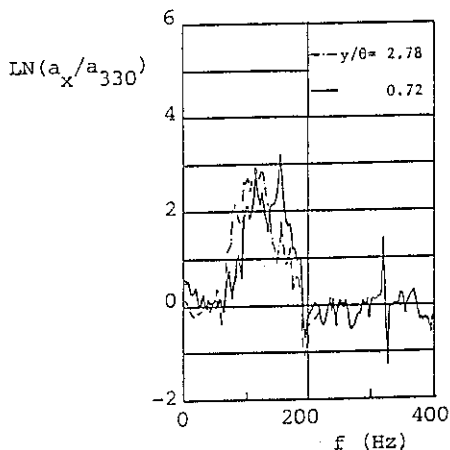

Figure 10. Amplification spectra reduced from spectra measured at different heights in the boundary layer at $x = 458$ mm.

Conclusions

A rather complete similar laminar and transitional flow field investigation has been described. Experimental mean velocity profiles showed good agree-

ment with Bola calculations. Amplification of disturbances was found in the predicted frequency range. Amplification factors were overpredicted with the LSL table while Cosal gave resonable agreement. The differences between the LSL table and Cosal are due to inaccuracies in the stability table of the first. This table will be updated in the future. Power distributions showed three maxima of which only two were predicted by linear stability calculations. The B-maximum which was relatively stronger represented at smaller frequencies seemed to be of a non-linear (subharmonic) nature.

REFERENCES
1. J.L. van Ingen, L.M.M. Boermans, J.J.H. Blom: Low speed airfoil section research at Delft University of Technology. ICAS-80-10.1, Munich, October 1980.

2. M.R. Malik: Finite difference solution of the compressible stability eigenvalue problem. NASA CR-3584, 1982.

3. J.P.F. Lindhout, G. Moek, E. de Boer, B. v.d. Berg: A method for the calculation of 3D boundary layers on practical wing configurations. Journal of Fluids Engineering, vol. 103, 1981.

4. H.U. Meier, U. Michel, H.P. Kreplin: The influence of windtunnel turbulence on the boundary layer transition. Perspectives in turbulence studies, symposium, DFVLR, Göttingen, editors: H.U. Meier and P. Bradshaw, Springer Verlag, May 1987.

5. U. Michel, E. Froebel: Lower limit for the velocity fluctuation level in windtunnels. Exp. in Fluids 6, 49-54, 1988.

6. F.J.M. Wubben: Experimental investigation of Tollmien Schlichting instability and transition in similar boundary layer flow in an adverse pressure gradient (Hartree $\beta = -0.14$). LR-report 604, Delft University of Technology, Department of Aerospace Engineering,1989.

7. Yu. S. Kachanov, V.V. Kozlov, V.Ya Levchenko: Non linear development of a wave in a boundary layer. Fluid dynamics 12, (translated from Izvestiya Akademii Nauk SSSR), 1978.

8. Yu. S. Kachanov, V.Ya. Levchenko: The resonant interaction of disturbances at laminar turbulent transition in a boundary layer. Journal of Fluid Mechanics 138, 1984.

9. D. Arnal: Diagrammes de stabilite des profils de couche limite auto-semblables, ecoulement bidimensionnel incompressible, sans et avec courant de retour. RT OA no. 34/5018, CERT, 1986.

10. T. Herbert, F.P. Bertolotti: Effect of pressure gradients on the growth of subharmonic disturbances in boundary layers. Proceedings of the conference on Low Reynolds number airfoil aerodynamics, edited by T.J. Mueller, UNDAS-CP-77B 123, Notre Dame, 1985.